DTIC FILE COPY (4)

# AD-A197 355

## REPORT DOCUMENTATION PAGE

| | |
|---|---|
| 1a. SECURITY CLASSIFICATION AUTHORITY | 1b. RESTRICTIVE MARKINGS |
| 2b. DECLASSIFICATION / DOWNGRADING SCHEDULE | 3. DISTRIBUTION / AVAILABILITY OF REPORT<br>Approved for public release and sale.<br>Distribution unlimited. |
| 4. PERFORMING ORGANIZATION REPORT NUMBER(S)<br>ONR Technical Report No. 9 | 5. MONITORING ORGANIZATION REPORT NUMBER(S) |
| 6a. NAME OF PERFORMING ORGANIZATION<br>University of Utah<br>6b. OFFICE SYMBOL (If applicable) | 7a. NAME OF MONITORING ORGANIZATION |
| 6c. ADDRESS (City, State, and ZIP Code)<br>Department of Chemistry<br>Henry Eyring Building<br>Salt Lake City, UT 84112 | 7b. ADDRESS (City, State, and ZIP Code) |
| 8a. NAME OF FUNDING / SPONSORING ORGANIZATION<br>Office of Naval Research<br>8b. OFFICE SYMBOL (If applicable) | 9. PROCUREMENT INSTRUMENT IDENTIFICATION NUMBER<br>N00014-85-K-0712 |
| 8c. ADDRESS (City, State, and ZIP Code)<br>Chemistry Program, Code 1113<br>800 N. Quincy Street<br>Arlington, VA 22217 | 10. SOURCE OF FUNDING NUMBERS<br>PROGRAM ELEMENT NO. / PROJECT NO. / TASK NO. / WORK UNIT ACCESSION NO |

11. TITLE (Include Security Classification)

The Behavior of Disk Electrodes: Optical Imaging of the Concentration Distribution over a Disk Electrode under Galvanostatic Conditions

12. PERSONAL AUTHOR(S)

J. Daschbach, S. F. Simpson, J. M. Harris, M. Fleischmann, and S. Pons

| 13a. TYPE OF REPORT | 13b. TIME COVERED | 14. DATE OF REPORT (Year, Month, Day) | 15. PAGE COUNT |
|---|---|---|---|
| Technical | FROM 9/87 TO 7/88 | July 15, 1988 | 16 |

16. SUPPLEMENTARY NOTATION

| 17 COSATI CODES | | | 18. SUBJECT TERMS (Continue on reverse if necessary and identify by block number) |
|---|---|---|---|
| FIELD | GROUP | SUB-GROUP | Real-time, CCD imaging of electrogenerated species |
| | | | |
| | | | |

19. ABSTRACT (Continue on reverse if necessary and identify by block number)

Attached.



| | |
|---|---|
| 20. DISTRIBUTION / AVAILABILITY OF ABSTRACT<br>☒ UNCLASSIFIED/UNLIMITED ☐ SAME AS RPT ☐ DTIC USERS | 21. ABSTRACT SECURITY CLASSIFICATION<br>Unclassified |
| 22a. NAME OF RESPONSIBLE INDIVIDUAL | 22b. TELEPHONE (Include Area Code) / 22c. OFFICE SYMBOL |

DD FORM 1473, 84 MAR — 83 APR edition may be used until exhausted. All other editions are obsolete.

SECURITY CLASSIFICATION OF THIS PAGE

88 7 26 089

OFFICE OF NAVAL RESEARCH

Contract N00014-85-K-0712

R&T Code 413a001---01
Replaces Old Task #056-123

Technical Report No. 9

# The Behavior of Disk Electrodes: Optical Imaging of the Concentration Distribution over a Disk Electrode under Galvanostatic Conditions

Prepared for publication in J. Electroanal.

by

J. Daschbach, S. F. Simpson, J. M. Harris, M. Fleischmann, and S. Pons

Department of Chemistry
University of Utah
Salt Lake City, UT 84112

July 15, 1988

# THE BEHAVIOR OF DISK ELECTRODES.

# OPTICAL IMAGING OF THE CONCENTRATION DISTRIBUTION OVER A DISK ELECTRODE UNDER GALVANOSTATIC CONDITIONS

John Daschbach, Stanley F. Simpson, Joel M. Harris,

Martin Fleischmann[1], and Stanley Pons*

Department of Chemistry
University of Utah
Salt Lake City, UT 84119
USA

[1]Department of Chemistry
The University
Southampton, Hants. SO9 5NH
ENGLAND

*To whom correspondence should be addressed.

**Abstract**

In this paper, we describe the theoretical and experimental determination of the integrated time dependent concentration distribution of an electrogenerated species over a disk electrode embedded in an insulated plane. We have derived this result for the case of constant applied flux (chronopotentiometry). The experimental technique used for observing the integrated concentration distribution over the electrode was imaging by a low noise charge coupled device camera with time and spatial resolution of approximately 20ms and 20μm respectively. The experiment demonstrates the contribution of the tertiary current distribution across the surface of the electrode.

## Introduction

There has been considerable interest recently in the behavior of microelectrodes because of their unique applications in electrochemistry (1-15). Due to the ease of fabrication and convenience of use, disk and ring electrodes are the most commonly used geometries. In addition to measurements in media of high resistance, small disk and ring microelectrodes have advantages for kinetic measurements since quasi spherical diffusion fields are established more rapidly than at line or band electrodes. These fields result in high rates of mass transport to the surface. As one application, therefore, depending on the size of the electrode, the kinetics of heterogeneous electron transfer reactions and of fast reactions in solution may be studied by *steady state* measurements.(16). Large disk electrodes (ca. 1mm or larger) generally will not demonstrate steady state conditions before convection dominates the mass transport.

Mathematical analysis and experimental results have indicated that the diffusion limited flux for fast heterogeneous reactions approaches very large values at the electrode-insulator boundary of embedded electrodes. The combined effects of finite rates of heterogeneous reactions and non-uniform distribution of potential and current across the electrode surface will limit the total reaction rate at the edges for real systems(1).

While there has been a variety of analytical and simulation methods developed for determining the complex transient electrochemical responses at finite disk electrodes (2-5,16-29), only recently have exact solutions been developed for a variety of steady state and transient techniques. Recently we reported the analyses of the responses for a variety of transient electrochemical experiments based on the properties of discontinuous integrals (1-5,16). In this paper, we develop the theory for the time dependent integrated concentration distribution of an electrogenerated species above a

finite disk electrode under constant flux conditions (chronopotentiometry) which is valid at all times for any size circular disk electrode. The predicted time dependent distribution is compared to the experimental response obtained from the *in situ* imaging the surface of a disk electrode with a charge coupled device (CCD) camera located above the plane of the electrode. The experiment is similar to that performed by Engstrom (30), in which an image of surface *flux* was obtained by photography at various times. We extend his results by performing the time and space dependent experiments *in situ*, and by comparing the results to an exact analysis of the constant flux model of the finite disk electrode. It is observed that the effects of non-uniform distribution of current (tertiary distribution) across the electrode distorts the predicted concentration distribution.

## Experimental

Concentration detection was made by an optical camera system based upon a charge coupled device (CCD). The detection system consisted of a front illuminated, uncoated Thomson CSF CCD chip (Model TH7882CDA, pixel size 23$\mu$m X 23$\mu$m, physical size 8.8mm x 13.2mm) housed in a cryogenic camera head (Model CH210, Photometrics, Ltd., Tucson, AZ), and operated at -120 C. Data were acquired via the associated readout electronics (Model CC200 and Model CE200, Photometrics, Ltd., Tucson, AZ), operated under GPIB control by a Compaq 386/20 host computer. Timing of optical detection was provided by an external circuit driving the camera head mounted shutter, which was synchronized with the electrochemistry. Simultaneous recording of the electrochemical current transients was accomplished with a Lecroy 9400 Digital Oscilloscope,and transferred to the host computer via the GPIB. The optical cell was a standard UV-VIS specular reflectance configuration, outfitted with a 7mm diameter platinum working mirror electrode which was illuminated by a quartz

halogen lamp. Wavelength control was accomplished with appropriate interference filters. The solution was 10mM benzophenone in 100mM tetra-n-butylammonium tetrafluoroborate in dry acetonitrile.

Chemicals.

Acetonitrile (Aldrich Gold Label) was used as received. Benzophenone (J.T. Baker Chemical Co., Phillipsburg, NJ) was recrystallized from hexane and dried under vacuum. Tetra-n-butylammonium tetrafluoroborate (TBAF, Chem-Biochem Research, Salt Lake City, UT) was used as received. All solutions were prepared and transferred under dry nitrogen.

## Theoretical Considerations

### General Time and Space Dependent Solution

We have previously solved the time dependent diffusion equation in circular cylindrical coordinates for a simple electrochemical experiment involving a single reactant and product (2-5):

$$A + e^- \rightleftarrows B \qquad [1]$$

The equation is

$$\frac{\partial C}{\partial t} = D \frac{\partial^2 C}{\partial r^2} + \frac{D}{r} \frac{\partial C}{\partial r} + D \frac{\partial^2 C}{\partial z^2} . \qquad [2]$$

where C is the concentration of the reactant or product, and r is the radial distance coordinate measured from the center of the disk electrode. We assume that the disk electrode is imbedded in the insulating plane $z = 0$. The initial condition for the experiment is

$$r > 0, \quad z > 0, \quad t = 0, \qquad C = C^{\infty} \qquad [3]$$

(where $C^{\infty}$ is the bulk concentration), and the boundary conditions are

$$0 \leq r < a, \quad z = 0, \quad t > 0, \quad D\left[\frac{\partial C}{\partial z}\right] = -Q.$$

$$r > a, \quad z = 0, \quad t > 0, \qquad D\left[\frac{\partial C}{\partial z}\right] = 0, \qquad [4]$$

for a constant flux (chronopotentiometric) experiment. In the previous work, (3), we obtained the general result (in Laplace space)

$$\bar{C} = \frac{C^{\infty}}{s} - \frac{Qa}{Ds} \int_0^{\infty} \exp[-f(\lambda,q)z] J_0(\alpha r) J_1(\alpha a) \frac{d\alpha}{f(\lambda,q)} \qquad [5]$$

where

$$q^2 = \frac{s}{D}. \qquad [6]$$

Here, s is the Laplace transformation variable, while

$$\alpha^2 = [f(\lambda,q)]^2 - q^2, \qquad [7]$$

and $J_0$ and $J_1$ are Bessel functions of the zeroth and first order respectively.

We rewrite [5] as

$$\bar{C} = \frac{C^{\infty}}{s} - \frac{Qa}{D} \int_0^{\infty} \exp[-(q^2 + \alpha^2)z] J_0(\alpha r) J_1(\alpha a) \frac{d\alpha}{s\,(q^2 + \alpha^2)^{1/2}} \qquad [8]$$

In the experiments described in this work, we record the integrated

concentration distribution over the entire region above the electrode surface

$$0 < z < \infty \qquad [9]$$

We therefore integrate [8] over all z

$$\int_0^\infty \bar{C}\, dz \; - \bar{C}_z - \frac{Qa}{D} \int_0^\infty\int_0^\infty \exp[-(q^2+\alpha^2)z] J_0(\alpha r) J_1(\alpha a) \frac{dz\, d\alpha}{s\,(q^2+\alpha^2)^{1/2}} \qquad [10]$$

$$- \frac{Qa}{D} \int_0^\infty J_0(\alpha r) J_1(\alpha a) \frac{d\alpha}{s\,(q^2+\alpha^2)}$$

$$- \; Qa \int_0^\infty J_0(\alpha r) J_1(\alpha a) \frac{d\alpha}{s(s + D\alpha^2)} \qquad [11]$$

We invert under the integral sign

$$\mathcal{L}^{-1}\left[\frac{1}{s(s + D\alpha^2)}\right] - \frac{1}{D\alpha^2}\left\{1 - \exp\left[D\alpha^2 t\right]\right\} \qquad [12]$$

to obtain

$$C\left[\frac{r}{a}, \frac{Dt}{a^2}\right] \; - \; Qa \int_0^\infty J_0(\alpha r) J_1(\alpha a) \frac{\left[1-\exp\left[-D\alpha^2 t\right]\right] d\alpha}{D\alpha^2}$$

$$- \frac{Qa}{D} \int_0^\infty J_0\left[\beta \cdot \frac{r}{a} \cdot \frac{a}{\ell}\right] J_1\left[\beta \cdot \frac{a}{\ell}\right] \frac{\left[1-\exp\left[-\beta^2\right]\right] d\beta}{\beta^2 \cdot \frac{a}{\ell}} \qquad [13]$$

where

$$\beta = \alpha \ell \qquad [14]$$

and

$$\frac{\ell^2}{a^2} = \left[\frac{Dt}{a^2}\right] \qquad [15]$$

Equation [13] is the integrated time dependent concentration distribution profile over the disk.

At sufficiently long times and small values of the flux, we do not observe a transition time and always reach the steady state value for a disk (16)

$$C_{Av} = C^{\infty} - \frac{8Qa}{3\pi D} . \qquad [16]$$

If Q is sufficiently large we observe a transition time as the surface concentration of the reactant approaches zero. For this condition and for any disk of radius a we have (3)

$$\frac{2Qa}{DC^{\infty}} \cdot \frac{\ell}{a}\int_0^{\infty}\left[J_1\left(\beta \cdot \frac{a}{\ell}\right)\right]^2 \operatorname{erf}(\beta)\frac{d\beta}{\beta^2}$$

$$= \frac{2Qa}{DC^{\infty}} \cdot \Phi_1\left[\frac{Dt}{a^2}\right] = 1 \qquad [17]$$

from which the transition time can be obtained. In the experiments described herein, we have maintained the flux at sufficiently low values so as not to reach a transition.

## Results and Discussion

The development of the time dependent integrated concentration distribution over a circular disk electrode of electrogenerated benzophenone ketyl anion in a constant flux (chronopotentiometric) experiment was recorded as described in the experimental section. Even though the total flux to the electrode is constant in time, the flux is not constant across the surface of the electrode. At a disk electrode, a non-linear current distribution will develop across the surface due to the discontinuity of the electrode surface at the electrode-insulator interface. At short times, the higher electric field strength at the edge of the disk compared to the interior planar portion will cause preferential migration of ions to the edge. The double layer at the edge is therefore charged at a faster rate than at the interior points, and electron transfer begins first at the edge. Migration of supporting electrolyte ions toward the edge will continue due to electrogeneration of ionic species of opposite charge there. As a result, there is further depletion of ions from regions over the interior of the the disk toward the edge causing further delay in the charging of the surface. This situation leads initially to higher concentrations of ketyl near the edge of the electrode. Figure 1 is a plot of the data obtained for the integrated absorbance profiles at 40, 100, 200, 300, 400, 500, and 1000ms, respectively. The integrated distributions in the Figure are a convolution of the concentration distributions predicted by equation [13] and those generated by the effects of the tertiary current distribution. Figure 1b are the predicted responses according to equation [13] using literature values for the diffusion coefficient. Figure 2 repesents differences in absorbances for various times. After approximately 100ms (determined by successive incremental subtractions), we find that the flux becomes essentially constant across the surface of the electrode. When this condition is attained, we predict and observe that the

intensity of the absorbance of the concentration profiles increases linearly with time across the surface, except near the edge where they to fall asymptotically toward the bulk value ($C_B = 0$). At long times, we predict that the concentration distribution will asymptotically decrease from the center of the disk since there is no flux at $z = 0$, $r > a$. This "flat" distribution will be observed at shorter times for small disks than at larger ones, Figure 3, and is a function of the parameter $a/(Dt)^{1/2}$, Equation [13]. We have pointed out that these profiles are similar to those in constant potential experiments in which there is heterogeneous kinetic control (1). As an illustration, the curve $a/(Dt)^{1/2} = 0.01$ corresponds to the integrated concentration profile developed in a chronopotentiometric response over a disk microelectrode of radius 0.1$\mu$m, 1 second after application of the constant flux Q ($D = 1.0 \times 10^{-5} cm^2 s^{-1}$), whereas the bottom curve ($a/(Dt)^{1/2} = 10.0$) corresponds to the integrated profile which has developed under the same experimental conditions after a microsecond. Alternately, for a 1cm radius electrode, the bottom curve corresponds to a time of $10^4$s ! For the experiments performed herein, therefore, we expect to observe a linear distribution of concentration above the electrode except very near the edge (after relaxation of the tertiary current distribution).

The nature of the experiment precludes accurate determination of integrated concentration distributions outside $r = a$. The reflection of light is specular from the electrode surface, whereas reflection from the insulator surface at $r > a$ is both diffuse and inherently less intense. An additional problem can arise due to the non-uniform lapping of edges at the metal-insulator boundary. Inhomogenieties across the boundary will always be present due to mechanical polishing. These points are much more obvious in experiments involving surface flux (30) (surface luminescence) imaging, and will be the subject of another report (31). As a result, the error in

determining the transmission becomes limited by the digitization accuracy of the instrumentation. We have therefore truncated the data at points $r > a$ since they are not significant. The observation of time dependent concentration and surface flux distribution profiles above the surface of small finite disk electrodes requires more sophisticated focussed imaging techniques and multichannel analysis techniques. In this context, it is interesting to compare the differences in the profiles for the cases of constant surface flux (chronopotentiometry) and constant average surface concentration (chronoamperometry). This point and applications to small electrode imaging will be reported shortly.

Acknowledgement

We thank the Office of Naval Research for support of this work.

References


1. M. Fleischmann, S. Pons, D.R. Rolison, and P. P. Schmidt, "Ultramicroelectrodes", Datatech Science, PO 435, Morganton, NC, 1987.

2. M. Fleischmann, J. Daschbach, and S. Pons, J. Electroanal. Chem., in press.

3. M. Fleischmann and S. Pons, J. Electroanal. Chem., in press.

4. M. Fleischmann and S. Pons, J. Electroanal. Chem., in press.

5. M. Fleischmann and S. Pons, J. Electroanal. Chem., in press.

6. P. Bindra, A. P. Brown, M. Fleischmann and D. Pletcher, J. Electroanal. Chem., 58 (1975) 31.

7. P. Bindra, A. P. Brown, M. Fleischmann and D. Pletcher, J. Electroanal Chem., 58 (1975) 39.

8. G. Gunawardena, G. J. Hills and B. Scharifker, J. Electroanal Chem., 130 (1981) 99.

9. A. M. Bond, M. Fleischmann, S. B. Khoo, S. Pons and J. Robinson, Extended Abstracts 165th Meeting of the Electrochemical Society, May (1984), Electrochemical Society, Pennington N.J., (1984).

10. R. M. Wightman and K.R. Wehmeyer, Anal. Chem., 57 (1985) 1989.

11. M. Fleischmann, J. Ghoroghchian and S. Pons, J. Phys. Chem., 89 (1985) 5530.

12. M. Fleischmann, J. Ghoroghchian, S. Pons and D. Rolison, J. Phys. Chem., 90 (1986) 6392.

13. J. Pons, J. Daschbach, M. Fleischmann, and S. Pons, J. Electroanal. Chem., 239 (1988) 427.

14. M. Fleischmann, S. Bandyopadhyay and S. Pons, J. Phys. Chem., 89 (1985) 5537.

15. M. A. Dayton, J. C. Brown, K. J. Stutts, and R. M. Wightman, Anal. Chem., 52 (1980) 946.

16. M. Fleischmann and S. Pons, J. Electroanal. Chem., 222 (1987) 107.

17. J. Heinze, J. Electroanal. Chem., 124 (1981) 73.

18. K. B. Oldham, J. Electroanal. Chem., 122 (1981) 1.

19. K. Aoki and J. Osteryoung, J. Electroanal. Chem., 122 (1981) 19.

20. B. Speiser and S. Pons, Can. J. Chem., 60 (1982) 1352.

21 B. Speiser and S. Pons, Can. J. Chem., 60 (1982) 2463.

22. K. Aoki, K. Akimoto, K. Tokuda, H. Matsuda and J. Osteryoung, J. Electroanal. Chem., 182 (1985) 281.

23. J. Cassidy and S. Pons, Can. J. Chem., 63 (1985) 3577.

24. T. Hepel, W. Plot, and J. Osteryoung, J. Phys. Chem., 87 (1983) 1278.

25. T. Hepel and J. Osteryoung, J. Phys. Chem., 86 (1982) 1406.

26. D. Shoup and A. Szabo, J. Electroanal. Chem., 140 (1982) 237.

27. K. Aoki and J. Osteryoung, J. Electroanal. Chem., 160 (1984) 335.

28. G. N. Watson, A Treatise on the Theory of Bessel Functions, 2nd Edition, Cambridge University Press, Cambridge (1948).

29. H. S. Carslaw and J. C. Jaeger, Conduction of Heat in Solids, Clarendon Press, Oxford (1959).

30. R. C. Engstrom, C. M. Pharr, and M. D. Koppang, J. Electroanal Chem. 221 (1987) 251.

31. J. Daschbach, S. Simpson, J. M. Harris, M. Fleischmann, and S. Pons, to be published.

**Figure legends**

Figure 1. (a). Integrated concentration distributions recorded (bottom to top) at 40, 100, 200, 300, 400, 500, and 1000ms, respectively. r and a are the radial coordinate and the radius (7mm) of the electrode respectively. The profiles are for electrogenerated benzophenone ketyl anion at a platinum electrode. (b). The predicted responses for the same times recorded in (a).

Figure 2 Differences in radial integrated concentration distributions across the disk electrode for the system described in Figure 1 at (bottom to top) 400-300ms, 500-300ms, and 1000-500ms respectively.

Figure 3. Plots of the dimensionless integrated concentration distribution across the surface of a disk electrode / insulator assembly as a function of the dimensionless parameter $a/(Dt)^{1/2}$ (Equation [13]).

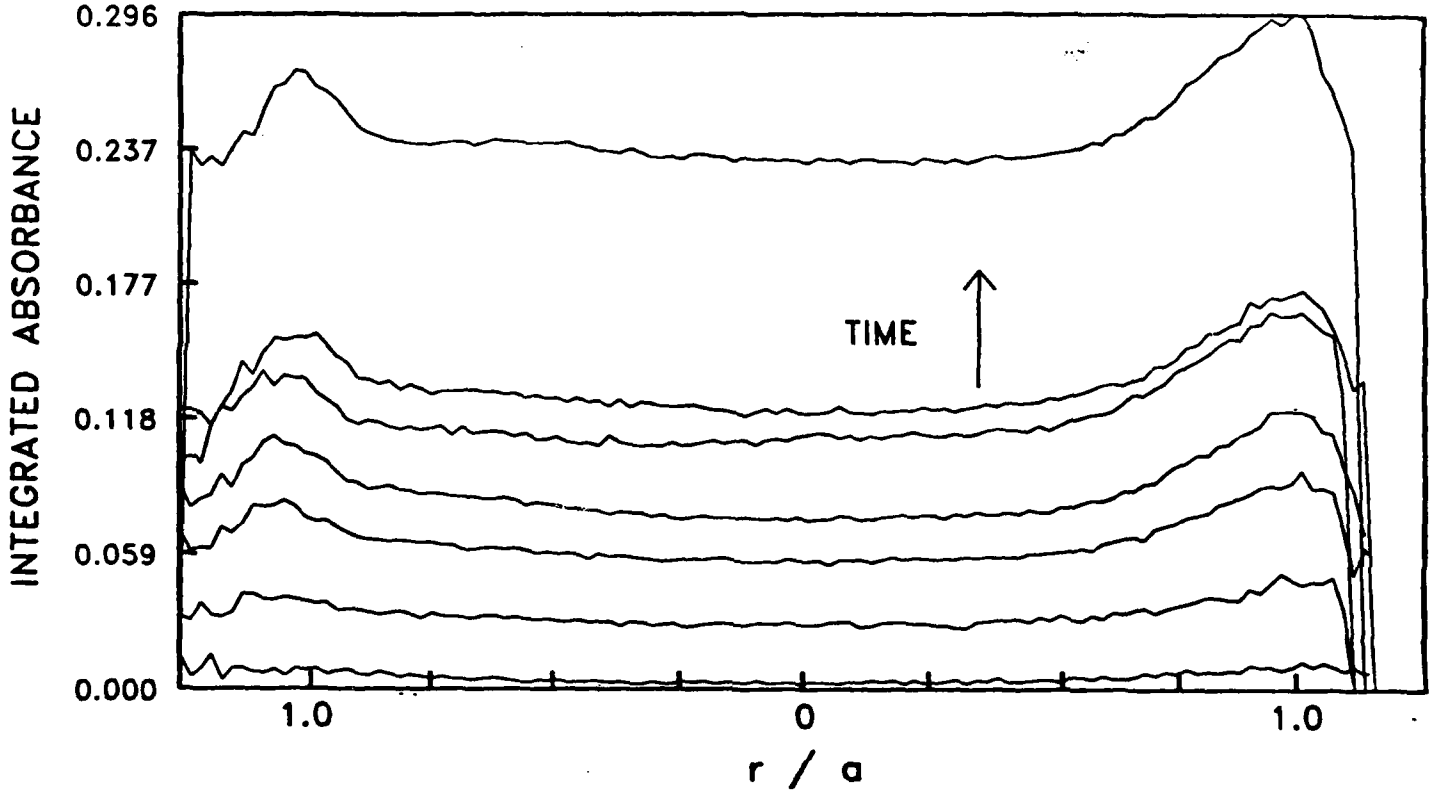
0.296
0.237
0.177
0.118
0.059
0.000
INTEGRATED ABSORBANCE
TIME
1.0
0
1.0
r / a

Fig 1a

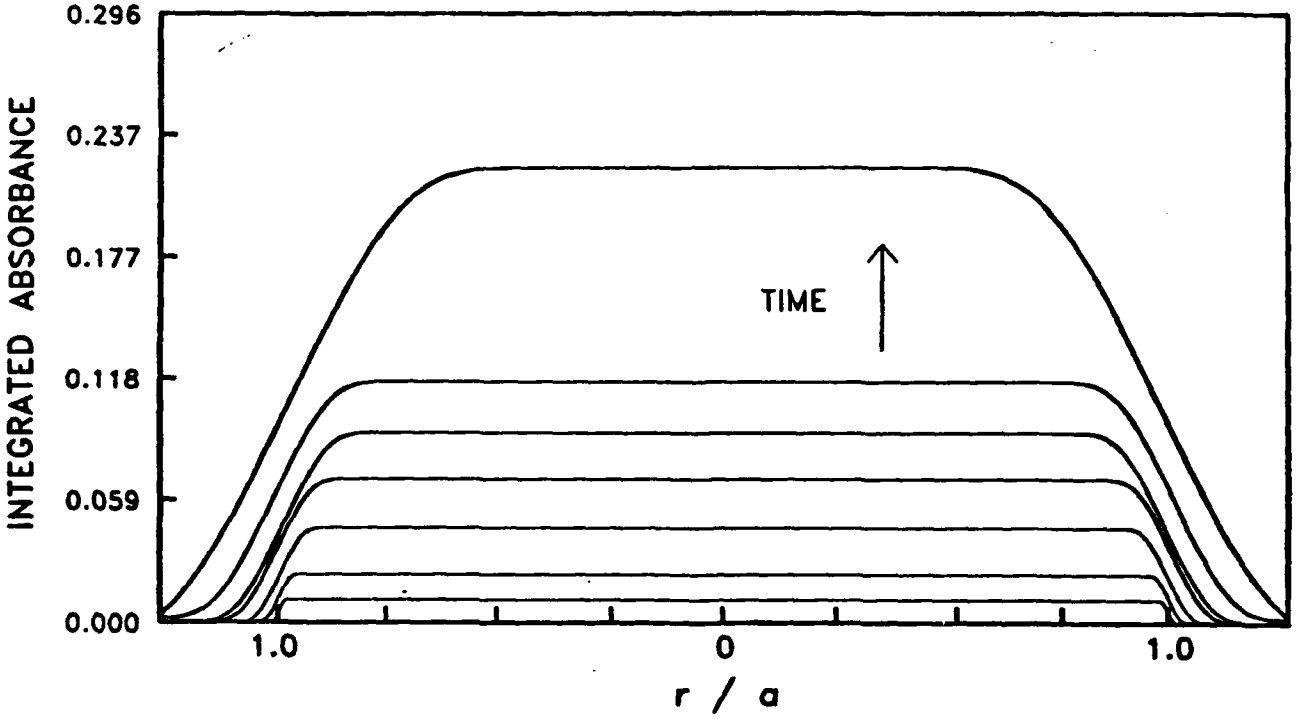
0.296
0.237
0.177
0.118
0.059
0.000
INTEGRATED ABSORBANCE
TIME
1.0
0
1.0
r / a

Fig 1b

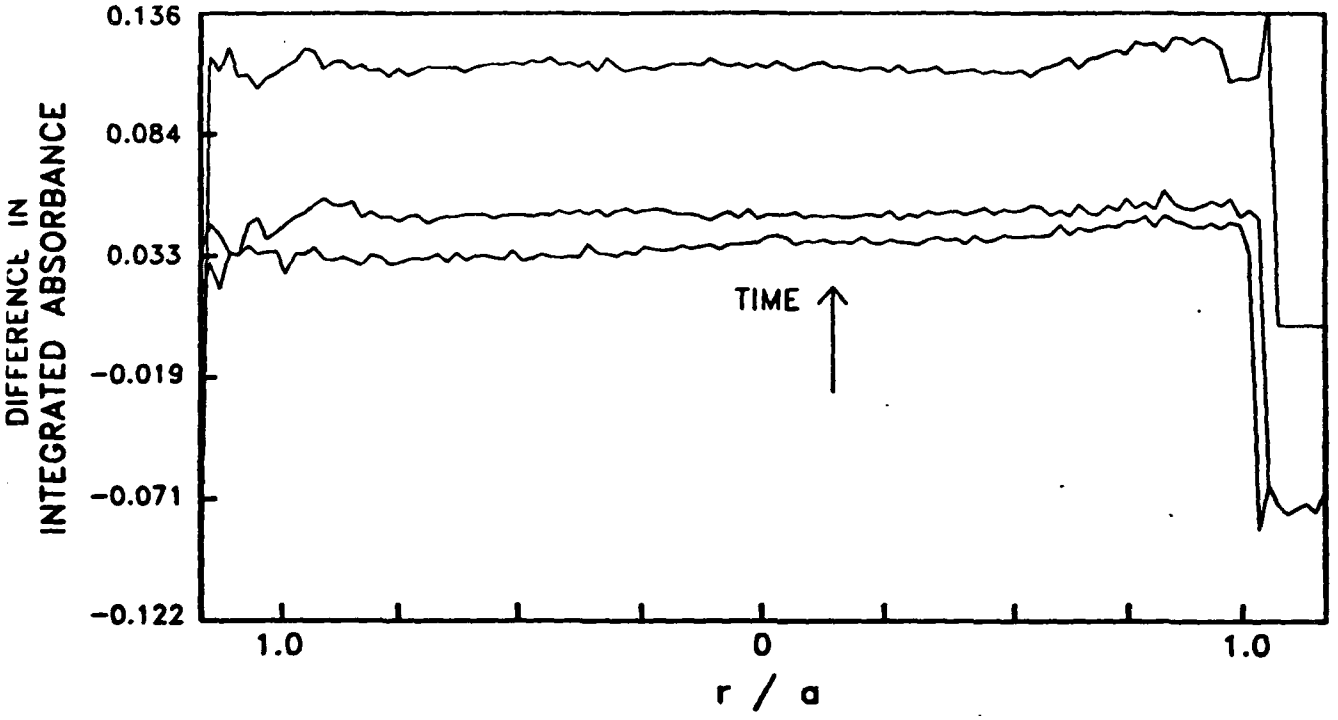
0.136
0.084
0.033
-0.019
-0.071
-0.122
DIFFERENCE IN
INTEGRATED ABSORBANCE
TIME
1.0
0
1.0
r / a

Fig 2

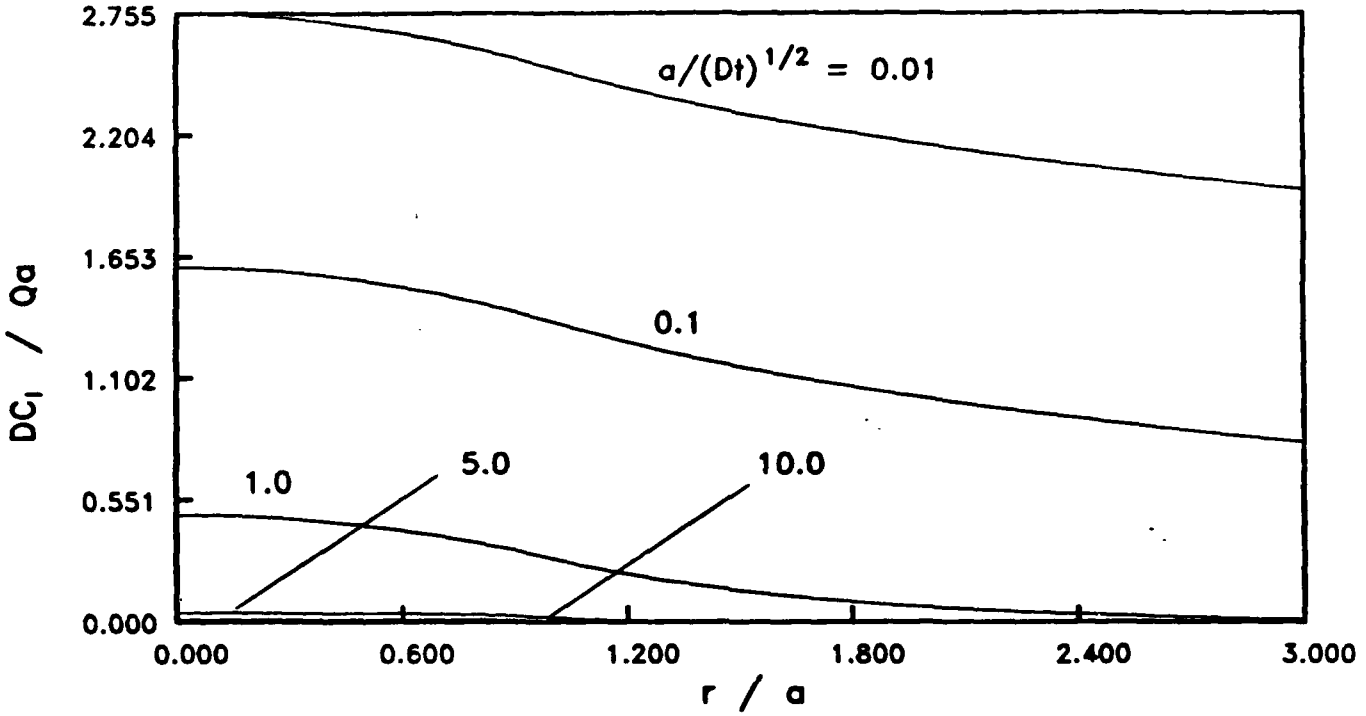
2.755
2.204
1.653
1.102
0.551
0.000
$DC_1 / Qa$
$a/(Dt)^{1/2} = 0.01$
0.1
1.0
5.0
10.0
0.000
0.600
1.200
1.800
2.400
3.000
r / a

Fig 3